Journal of Robotics and Control (JRC)
Volume 6, Issue 3, 2025
ISSN: 2715-5072, DOI: 10.18196/jrc.v6i3.25756

Robust Speed and Torque Control of DC Motor with Cuk Converter Using PI and SMC

Mohammed Albaker Najm Abed [1*], Dheyaa Shiltagh Shanan [2], Zinah Hayder Hammoodi Alhussein [3*]
[1, 2, 3] Computer Technology Engineering, Al_Taff University College, Karbala, Iraq
Email: [1] e09163265@s.uokerbala.edu.iq, [2] cse.21.18@grad.uotechnology.edu.iq , [3] zinah.alhusseini@altuff.edu.iq
*Corresponding Author

***Abstract*—Robust speed and torque control of a DC motor powered by a DC/DC converter has become widespread attention recently. This research examines the Cuk converter's effectiveness in powering the DC motor using proportional-integral (PI) and sliding mode control (SMC) under three operating scenarios: variable speed (1600-500 rpm) and constant torque (20 N.m), constant speed(600 rpm) and variable torque (20-40 N.m), and variable speed (500-100 rpm) and variable torque (20-40 N.m). The research aims to provide accurate motor speed and torque control to enhance motor operations. PI and SMC controllers were constructed to investigate how the system operated in different scenarios, mathematical models were made, and Matlab/Simulink modeling was used. The performance parameters measurements are the speed and torque tracking response, armature current, and the output voltage from the Cuk converter with their total harmonic distortions (THDs). The results showed that SMC performed PI in speed and torque tracking and had fewer fluctuations under all scenarios. The SMC controller had a lower overshoot of 0.05 while PI was 0.75, and a settling time of SMC 0.5 seconds is less than the PI controller's 25 seconds in tracking speed and torque. For output converter voltage and armature current, the THD of the PI controller was 0.2441 and 0.3857, respectively, but the THD of SMC was reduced to 0.0833 and 0.0921. lower THD in SMC leads to smoother waveforms and less electromagnetic interference, resulting in faster responses, fewer overshoots, and improved speed and torque. The SMC with Cuk converter was the best control method for the DC motor drive applications, providing increased performance, efficiency, and decreased system losses.**

Keywords—DC Motor Control; Speed Control; Torque Control; Nonlinear Control Techniques; PI Controller; Sliding Mode Control (SMC); Cuk Converter-Fed DC Motor; Matlab/Simulink.

I. Introduction Industrial Automation and Robotics to Renewable Energy System

A DC motor is one of the types of electric motors. DC motor adaptability, controllability, and simplicity of use make them popular in various applications. For applications including industrial automation and robotics to renewable energy systems, accurate DC motor speed and torque control is essential to achieving optimal performance and meeting stringent specifications [1], [2]. Numerous control systems have been created to achieve this goal, each with advantages and disadvantages [3]-[5].

Users usually utilize PI controllers because of their simplicity and ease of use. The motor input is modified using PI parameters based on the difference between reference and measured speed [6]. The possible shortage of resiliency of PI controllers to PI parameter changes can lead to shorter responses and higher steady-state errors. To improve transient response and minimize overshoot, PID controllers add a derivative component to PI control [7]. PID controllers must be accurately tuned to prevent instability because they are noise-sensitive [8], [9]. While PID and PI are crucial for applications of DC motors, it is essential to understand their limitations. Determining whether to utilize a PID controller and how to tune it efficiently requires careful evaluation of the system dynamics, noise characteristics, and performance needs [10]-[12].

Sliding Mode Control (SMC) is a dependable control technique that drives the system trajectory into an initial sliding surface. SMC's advantages include finite-time convergence, fast response, and durability in perturbation and parameter changes. [13]. Chattering, or high-frequency oscillations in control signals, can be harmful and call for the right mitigation actions [14]. Utilizing DC/DC converters to power DC motors has recently become one of the practical solutions to the problem of regulating DC motors, which is characterized by significant tracking speed and torque variations, high THD, power losses, and energy consumption from the motor when utilizing standard control techniques [15], [16]. SMC can further enhance the motor drive's efficiency and stability when combined with the Cuk converter, a DC-DC converter topology that provides continuous input and output currents [17]-[19].

This study compares the effectiveness of PI and SMC controllers for DC motor speed control with a CUK converter [20], [21]. Their efficacy in achieving precise control under different operating conditions is assessed by comparing speed and torque tracking response, armature current, output voltage, and THD of both armature current and voltage [22].

While it controls the voltage sent to the motor, recently, DC/DC converters are crucial for motor drive systems. Numerous topologies are frequently used, each having unique properties and applicability for specific uses. When the output voltage exceeds the input voltage, buck converters [23], [24], boost converters [25], and Buck-boost converters [26]. Cuk converters can simplify filter design and increase efficiency because, like buck-boost converters, they provide both step-up and step-down capabilities while preserving continuous input and output currents [27], [28]. Cuk converters are frequently chosen when continuous input and output currents are required, like in applications where minimal output ripple is crucial [29], [30].

The necessary voltage conversion ratio, input and output voltage levels, required current, and desired efficiency all impact the DC/DC converter selection [31]. For instance, a buck converter would be ideal if the motor runs at a lower voltage than the available power source [32]. On the other hand, if a larger voltage is needed, a boost or buck-boost or Cuk converter converter would be required [33].

Pulse Width Modulation (PWM) Control is the most popular control method for Cuk converters and is the primary method utilized for these devices [34]. Changing the output voltage, PWM control modifies the duty cycle of the switching device, which is usually an IGBT or MOSFET [35], [36]. The output voltage is regulated by varying the switches, which also controls the quantity of energy transported from the input to the output. The error signal is then processed by a controller that generates the PWM-controlled signal for the converter switch [37], [38]. SMC offers significant control and improved dynamics performance for CUK converters [39]. A CUK converter powering a DC motor performs noticeably better when using SMC, producing a steady,low-ripple output voltage [40]. It is made possible by SMC is strong management of disruptions and capacity to reduce switching losses. SMC explicitly lowers harmonic distortion and voltage oscillations, giving the motor a cleaner power source [41]-[44].

The findings of this research have broad implications for various applications where precise and robust DC motor control is essential [45]. SMC can maximize electric vehicles' motor efficiency and battery life by reducing losses and ensuring smooth operation under fluctuating speed and torque demands. SMC's capacity to manage disruptions and sustain optimal energy conversion efficiency in changing climatic conditions might benefit renewable energy systems, including solar trackers and wind turbines.

By demonstrating the better performance of SMC in terms of speed and torque tracking precision, current and voltage ripple, and THD, the research contribution sets a performance baseline for DC motor drives with Cuk converters. Future studies and advancements may use that standard as a guide.

The organize the rest of the paper: Section 2 shows the methodology and mathematical model, including the DC motor, CUK converter, SMC, and PI controller. Section 3 shows the numerical results of the simulation for each scenario along with a description. Section 4 outlines the research results, future works, and references.

II. METHODOLOGY

A. DC Motor

One essential part of a drive system powered by a Cuk converter and managed by a PI or SMC controller is the DC motor in concern. To assess the effectiveness of the controllers, this motor is put through several operating scenarios, such as variable speed and constant torque, constant speed and variable torque, and variable speed and variable torque. The Cuk converter, which offers a controlled voltage source, affects the motor's operation. The choice of controller (PI or SMC) significantly affects the motor's behavior, particularly in speed tracking accuracy, torque regulation, and current and voltage ripple. The described DC motor is a powerful machine with 5 horsepower (HP) rated power output. It operates on a 240-volt supply and spins at a nominal speed of 1750 revolutions per minute (RPM). The field winding, which generates the magnetic field necessary for motor operation, is excited by a separate 300-volt supply. The mathematical model of the DC motor is given in [46]. Table I shows the DC motor parameters.

TABLE I. DC MOTOR PARAMETERS

Parameter Type	Value
Armature Resistance	2.581 ohms
Armature Inductance	0.028 H
Field Resistance	281.2 ohms
Field Inductance	156 H
Mutual Inductance	0.9483 H
Total Inertia	0.02215 kg.m^2
Viscous Friction Coefficient	0.002953 N.m.s
Friction Torque	0.5161 N.m

B. Cuk Converter

A Cuk converter is a DC-DC converter that maintains constant input and output currents while stepping up and down voltage. Energy is transferred between the input and output levels via two inductors and capacitors [47], [48]. Beneficial Impact on DC Motors:

When powering a DC motor, the Cuk converter has the following advantages:

a) Even when load conditions fluctuate, the converter's ability to regulate the motor voltage supply ensures consistent operations [49].

b) The duty cycle of the converter switch can be adjusted to modify the output voltage, which has an immediate effect on motor speed [50], [51].

c) The constant input and output currents may contribute to higher efficiency when compared to other converter topologies [52]. That feature simplifies filter design and reduces the size of the input and output capacitors. The effective filtering of the two inductors results in a cleaner output voltage. Due the Cuk converter can step up and down voltage, it can be used in a variety of applications. The steady currents and less ripple could lead to a higher efficiency than conventional converter [53], [54].

Although it can both increased or decreased voltage, Cuk and buck-boost converters differ in a few significant respects:

a) The Cuk converter uses two insuctors and a capacitor, while the buck-boost converter uses just one inductor.

b) The Cuk converter provides continuous input and output currents, whereas the buck-boost converter has discontinuous input or output current s depending on the operating mode.

c) Because of the extra filtering that the second inductor provided, the output ripple of the Cuk converter is typically lower [55].

The DC-DC Cuk converter circuit, shown in Fig. 1, comprises two capacitors (C1 and C2) and two inductors (L1 and L2). The converter's input and output voltages are denoted by E and v2, an active switch by M, a freewheeling diode by D, and load resistance by R. The switch M operates in the ON state ($u=1$) and OFF state ($u=0$) [29]. Cuk converter parameters shown in Table II.

TABLE II. CUK CONVERTER PARAMETERS

Parameter Type	Value
First and Second Inductance (L1, L2)	200×10^{-6} H
C1	200×10^{-6} F
C2	20×10^{-6}F
Input Voltage (Vin)	120 V

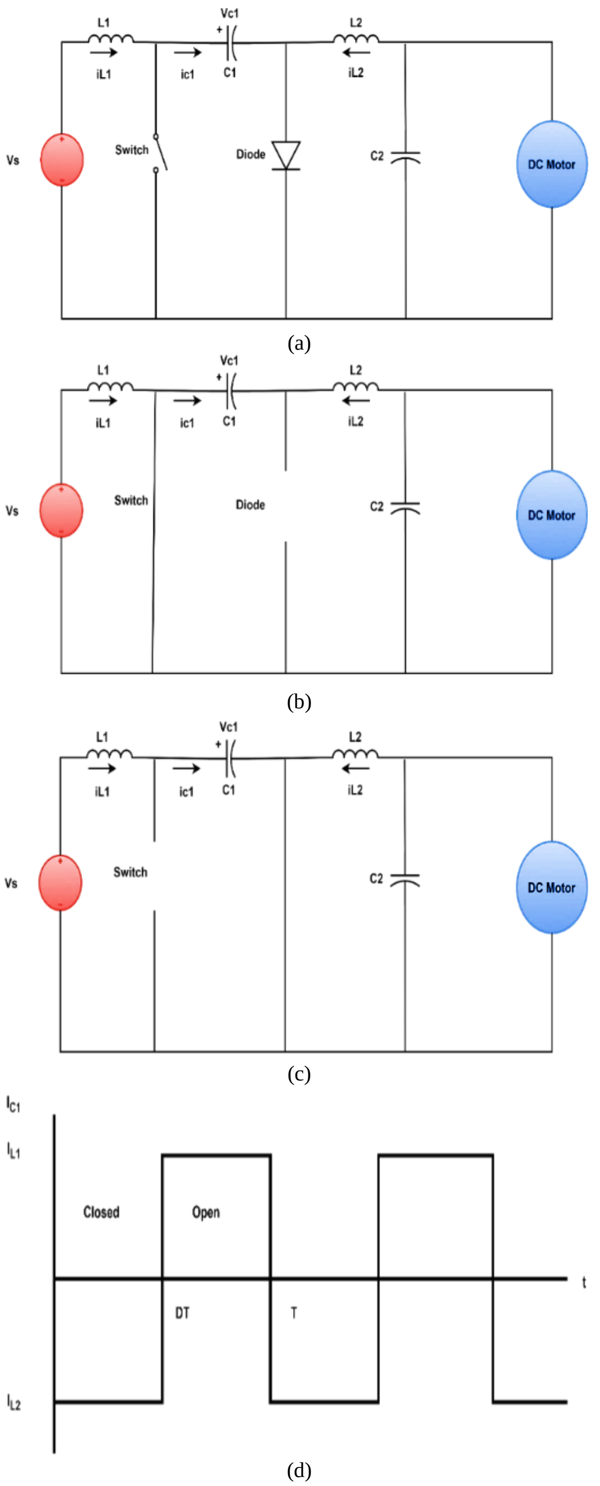

Fig. 1. The ´ Cuk converter. (a) circuit; (b) equivalent circuit for the switch closed; (c) equivalent circuit for the switch open; (d) current in L1 for a large inductance

The equations (1)-(4) represent the averaged state-space model of the Cuk converter. This model describes the dynamic behavior of the converter by relating the rates of change of inductor currents (i_1, i_2) and capacitor voltages (v_1, v_2) to the input voltage (E), the duty cycle (u), and the circuit parameters (L_1, L_2, C_1, C_2, R). Below is the averaged model of the state-space equations created while the switch was in both the ON and OFF states.

$$\frac{di_1}{dt} = \frac{1}{L_1}[E-(1-u)v_1] \tag{1}$$

$$\frac{di_2}{dt} = -\frac{1}{L_2}[uv_1+v_2] \tag{2}$$

$$\frac{dv_1}{dt} = \frac{1}{C_1}[ui_2+91-u)i_1] \tag{3}$$

$$\frac{dv_2}{dt} = \frac{1}{C_2}[i_2-\frac{v_2}{R}] \tag{4}$$

Where i_1 is the current through L_1, i_2 is the current through L_2, v_1 is the voltage across C_1, v_2 is the voltage across C_2. The compact matrix in equations (5) and (6) represents the state-space model. Designing and analyzing control systems can benefit from the model.

$$\dot{X} = \begin{bmatrix} 0 & 0 & \frac{-(1-u)}{L_1} & 0 \\ 0 & 0 & \frac{-u}{L_2} & \frac{-1}{L_2} \\ \frac{(1-u)}{C_1} & \frac{u}{C_1} & 0 & 0 \\ 0 & \frac{1}{C_2} & 0 & \frac{-1}{RC_2} \end{bmatrix} \begin{bmatrix} i_1 \\ i_2 \\ v_1 \\ v_2 \end{bmatrix} + \begin{bmatrix} \frac{1}{L_1} \\ 0 \\ 0 \\ 0 \end{bmatrix} [E] \tag{5}$$

This equation describes the dynamics of the state vector (X). The system dynamics, which rely on the duty cycle (u), are represented by the matrix $A(u)$. The input voltage (E) and the state vector dynamics are related by the matrix $B(u)$.

$$Y = [0 \quad 0 \quad 0 \quad 1] \begin{bmatrix} i_1 \\ i_2 \\ v_1 \\ v_2 \end{bmatrix} + [0]E \tag{6}$$

The output vector (Y) is described by this equation. The input voltage (E) is related to the output by matrix D, while the state vector (X) is related to the output by matrix C. The ON and OFF state-space equations are obtained by letting u = 1 (or) 0 in (5) and (6), respectively. Design of Cuk converter parameters:

Equations (7)-(12) provide guidelines for designing the Cuk converter parameters. Kirchhoff's voltage law determines the average voltage across C_1 in the DC-DC Cuk converter working in CCM across the outermost loop. Equation (7) relates the output voltage (V_o) to the input voltage (V_s) and the duty cycle (D). It shows that the Cuk converter can step-up or step-down the voltage depending on the duty cycle.

$$V_o = -V_s(\frac{D}{1-D}) \tag{7}$$

Equation (8) describes the output voltage ripple, which is influenced by the duty cycle (D), inductor L_2, capacitor C_2, and switching frequency (f).The negative symbol indicates an output and input polarity reversal. Note that the L_2, C_2, and R components of the production are arranged similarly, and that the inductor current has the same form as the buck converter. Therefore, the ripple, or variation in output voltage, is the same as for the buck converter:

$$\frac{\Delta V_0}{V_0} = \frac{1-D}{8L_2C_2f^2} \tag{8}$$

Equations (9)-(10) describe the inductor current ripple, which is influenced by the duty cycle (D), input voltage (V_S), switching frequency (f), and inductors L_1 and L_2.The inductor current varies when the switch is closed at the time interval DT.

$$\Delta i_{L1} = \frac{DV_s}{fL_1} \tag{9}$$

The change in i_{L2} is then:

$$\Delta i_{L2} = \frac{DV_s}{fL_2} \tag{10}$$

Equations (11)-(12) provide the minimum inductor values required to maintain continuous current flow. For the inductors to supply continuous current, The current change must be less than half of the average current. These are the smallest inductor sizes needed to maintain a steady current.

$$L_{1,min} = \frac{R(1-D)^2}{2Df} \tag{11}$$

$$L_{2,min} = \frac{(1-D)R}{2f} \tag{12}$$

C. *Slide Mode Control*

A DC motor powered by a Cuk converter has its speed and torque controlled using SMC [56]. SMC performs exceptionally well in this application because of its inherent resilience to perturbations and parameter changes, which are essential for maintaining accurate motor control [57], [58]. The switching pattern of the Cuk converter's power electronic switch is determined by a control signal produced by the SMC algorithm [59]. Even in the event of external disruptions or variations in load situations, SMC guarantees quick and precise monitoring of the intended speed and torque setpoints by dynamically modifying the duty cycle and switching frequency in response to real-time feedback from the motor's speed and current sensors [60].

To implement the SMC, we first model the system as a regulatory system synthesizing the hyperplane described in the equation [57], [58].

$$\dot{X} = Ax + Bu \tag{13}$$

Here, X represents the state vector, A the system matrix, B the input matrix, and u the control input. The suggested controller's sliding surface must meet:

$$s = Cx \tag{14}$$

where C is a matrix chosen to define the sliding surface. Differentiating the equation above and substituting $\dot{X}$, we get:

$$C\dot{X} = CAx + CBu = 0 \tag{15}$$

When the equation above is rearranged, it gets

$$CBu = -CAx \tag{16}$$

The corresponding open-loop linear control is provided by the hyperplane C, which is chosen so that $CB \neq 0$.

$$U_{eqv} = -(CB)^{-1}CAx = -Kx \tag{17}$$

The closed-loop system's equation while sliding is as follows:

$$\dot{X} = (A - BK)x \tag{18}$$

Implementation and Parameter Tuning:

A digital signal processor (DSP) was used to implement the SMC in the experimental arrangement. The average state-space model of the DC motor and CUK converter, taking into account the mechanical and electrical characterstic, was used to creat the matrix A and B. The sliding surface matrix C components were slected according to the system is bandwidth and settling time requirements to guarantee stability and the intended dynamic performance. Equation (17) was then used to calculate the gain matrix K.

To accurate-tune the SMC parameters, it used both analytical and experimental validation techniques: first, the sliding surface was designed according to the desired bandwidth and settling time of the system; next, the gain matrix K was computed; finally, the controller's performance was assessed through simulations the parameters were experimentally adjusted by monitoring the system in response to step changes in the speed and load disturbance; interactively, the parameters were adjusted to minimize overshoot, settling time, and steady-state error while making sure chattering remained within acceptable bounds.

Specifically, the elements of matrix C were adjusted to achieve a balance between fast convergence and chattering reduction. The gains in matrix K were fine-tuned to optimize the system's transient response and disturbance rejection. Then, under the identical operating conditions, the performance of the PI controller and the tuned SMC controller were contrasted.

Fig. 2 shows the SMC for the Cuk converter. The speed control system for a DC motor driven by a Cuk converter utilizing SMC is depicted in the block diagram [56]. The "Reference Speed" represents the desired motor speed, while the "Measured Speed" is the actual motor speed obtained through sensors. These signals are compared using a subtractor, and the resulting error is fed into the SMC block. The SMC block processes this error and generates a control signal. A "Gain" block then amplifies this control signal. The "Sawtooth Generator" produces a triangular waveform compared with the amplified control signal using a "Pulse" comparator. The output of the comparator is a pulse width modulated (PWM) signal, which drives the Cuk converter's switch, thereby controlling the motor's speed.

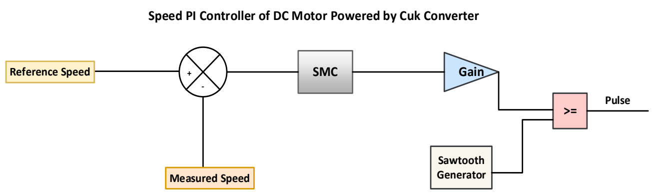

Fig. 2. Speed Control Block Diagram with SMC for a Cuk Converter-Fed DC Motor

D. PI Controller

A DC motor driven by a Cuk converter has its speed and torque controlled by a proportional-integral (PI) controller [61]. A popular linear control method, the PI controller compares the intended motor speed and torque with the actual values to provide an error signal [62], [63]. The PI algorithm processes this error signal and determines the proper duty cycle for the power electronic switch of the Cuk [64]. The PI controller efficiently changes the voltage and current delivered to the motor by varying the duty cycle, which regulates the motor's speed and torque [65]. Although PI controllers are typically easier to construct than SMC, they may not be as resilient to shocks and parameter changes [66]. It may result in more substantial steady-state errors and slower reaction times under difficult operational circumstances [67], [68]. The transfer function for the PID controller is given in (19):

$$\frac{C(s)}{E(s)} = Kp + Ki\,\frac{1}{s} + Kds \tag{19}$$

where K_p is the proportional constant gain and, E(s) is the error signal., The gain of the integration constant is represented by K_i, and its output is represented by C(s). Fig. 3 shows the PI controller of the Cuk converter.

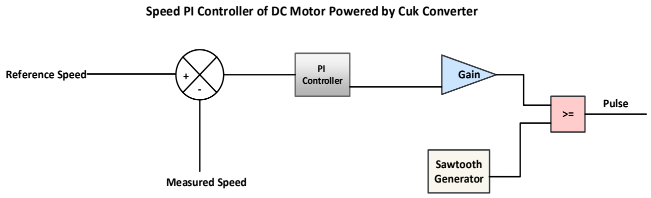

Fig. 3. Speed Control Block Diagram with PI for a Cuk Converter-Fed DC Motor

Fig. 4 provides a summary of the suggested system's complete block diagram. A closed-loop speed control system for a DC motor driven by a Cuk converter is shown in the block diagram [69]. The "Reference Speed" represents the desired motor speed. The "SMC/PI Controller" block, which can be either a SMC or a PI Controller, compares the "Reference Speed" with the "Measured Speed" obtained from the motor. Based on this comparison, the controller generates a "Duty Cycle" signal [70]. This signal dictates the switching pattern of the "Cuk Converter," which regulates the voltage supplied to the "DC Motor." The "Load" represents the external mechanical load on the motor [71]. The "Voltage Source" supplies the Cuk converter with its input power. The loop is closed and continuous speed management is made possible by feeding the "Measured Speed" back to the controller.

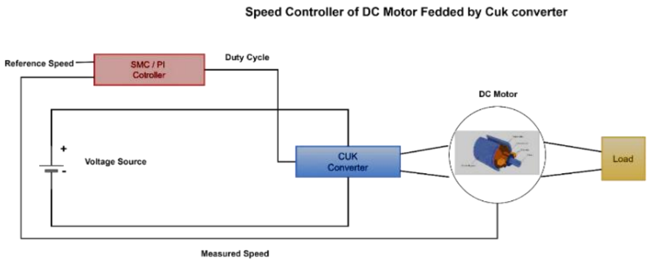

Fig. 4. Closed-Loop Speed Control System for a DC Motor Powered by a Cuk Converter

Fig. 5 shows the flowchart of PI and SMC for DC motor control with the Cuk converter. It provides a detailed explanation of each methodology stage.

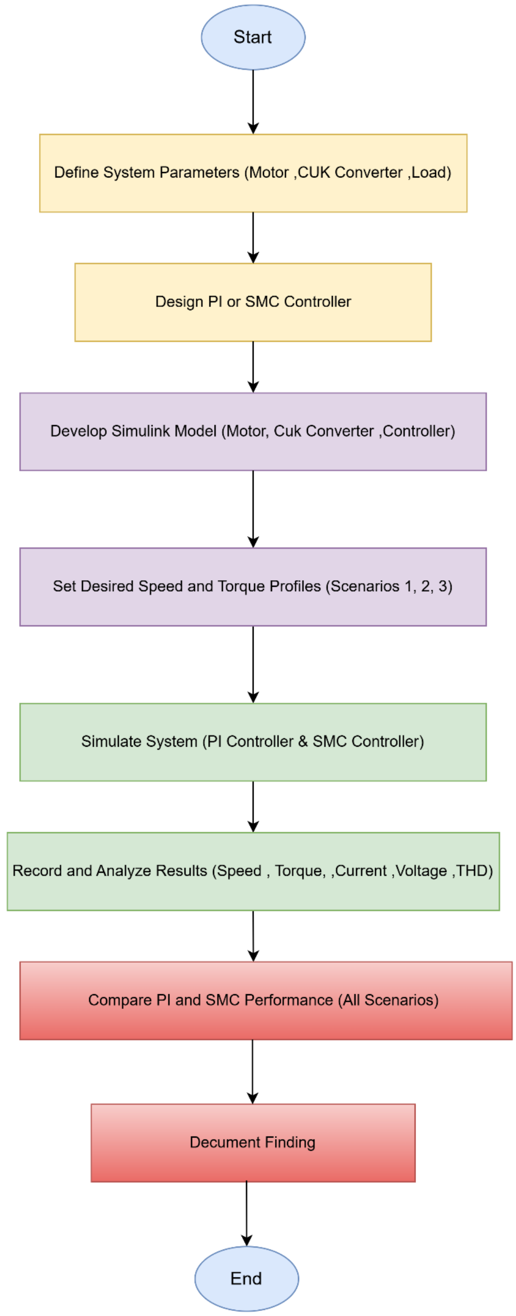

Fig. 5. Flowchart of PI and SMC for DC Motor Control with Cuk Converter.

III. Results and Discussion

Three scenarios will be used to compare the SMC and PI controllers. Variable speed and constant torque are present in the first situation. The second scenario is constant speed and variable torque. The third is scenario variable speed and torque. Analyze the simulation results, focusing on the following parameters:

- Output Speed: Analyze the settling time, tracking accuracy, and speed responsiveness.

- Output Torque: Examine the motor's capacity to provide the required torque in various scenarios.

- Cuk Converter Output Voltage: Examine the converter's ability to regulate voltage.
- Armature Current: Keep an eye out for variations in current and the possibility of overcurrent scenarios.
- THD for current and voltage: Examine the THD of the voltage and current.

A. *First Scenario*

Fig. 5 shows the first scenario response of the DC motor with both controllers. Fig. 5 (a) depicts the speed response of a DC motor under two control strategies, PI and SMC, across a 50-second interval. The reference speed, shown in yellow, follows a step-wise pattern, starting at approximately 1500 rpm, dropping to 500 rpm at 10 seconds, then increasing to 700 rpm at 20 seconds, and finally reaching 800 rpm at 30 seconds, maintaining this until 50 seconds.

The SMC controller, represented by the blue line, closely tracks the reference speed. It exhibits a rapid rise time with minimal overshoot at each step change, settling quickly to the new reference value. For instance, at the initial step to 1500 rpm, SMC reaches the reference within approximately 1 second. Similarly, at 10 seconds, it rapidly drops to 500 rpm with a sharp transition.

The PI controller, shown in red, displays significant oscillations and overshoots around the reference speed. At the initial step, it overshoots to approximately 3000 rpm before oscillating and settling around the reference. At 10 seconds, it exhibits a sharp undershoot before stabilizing. Throughout the 50-second interval, the PI controller shows persistent oscillations, particularly noticeable in the magnified inset, where it fluctuates between approximately 1580 rpm and 1620 rpm around the 1600 rpm reference.

Fig. 5 (b) displays torque response over 50 seconds, with a reference torque of approximately 20 N.m. The SMC (blue) maintains torque near 20 N.m with minor fluctuations. The PI (red) exhibits significant torque oscillations, ranging from approximately 15 N.m to 25 N.m, particularly prominent in the magnified inset. At 10 seconds, PI shows a sharp negative spike. At 20 and 30 seconds, PI displays brief, large positive spikes. SMC's torque remains stable, with fluctuations under 1 N.m, while PI's fluctuations exceed 5 N.m. SMC's superior performance is due to its robustness against disturbances and ability to maintain a stable sliding mode, effectively rejecting the impact of speed variations on torque. Fig. 4 (c) shows the armature current response in the first scenario, where PI and SMC controllers control the DC motor.

The armature current graph spans 50 seconds, maintaining a consistent pattern throughout. The SMC shows a steady current of around 20 Amps, with minor fluctuations within a 1 Amp range. The PI controller exhibits significant current oscillations between 18 and 24 Amps, with occasional sharp spikes reaching 0 and 40 Amps. The PI current fluctuates between roughly 23 and 26 amps, as the zoomed figure shows. SMC maintains a stable current with minimal ripple, while PI displays substantial fluctuations and spikes, indicating less stable current regulation. Based on the initial scenarios, the voltage response from the Cuk converter for both PI and SMC controllers is shown in Fig. 5(d). There are significant ripple and voltage variations in the PI. The increased switching activity brought on by the PI controller control signal is probably the cause of these oscillations.

The voltage wave from the SMC is substantially smoother and has less ripple. It suggests that the SMC controller produces a control signal that reduces the Cuk converter switching activity, leading to a more steady and even output voltage.

B. *Second Scenario*

Fig. 6 shows the motor response of the second scenario. Fig. 6 (a) shows the speed response. The speed response curve illustrates SMC's power in this specific scenario. Even under fluctuating torque loads, SMC can maintain a desired constant speed with much greater precision than the PI controller thanks to its robustness to disturbances, quicker response time, and chattering reduction capabilities.

Fig. 6 (b) shows that the SMC performs better torque tracking than the PI controller. The inherent robustness of SMC enables it to efficiently offset the impacts of load fluctuations and maintain the required torque level with higher precision. The SMC controller maintains the reference torque with substantially less deviation and oscillation. This rapid response helps to minimize the impact of load variations on the motor's torque output.

Fig. 6(c) demonstrates the motor's armature current response. The current change depends on variable torque load. SMC maintains a relatively stable current around 20 Amps until 10 seconds, then rises to 28 Amps at 15 and 36 Amps at 30 seconds, maintaining this level until 50 seconds. Fluctuations are minimal, staying within 1 Amp of the steady state. PI exhibits similar trends but with significant oscillations. From 0 to 10 seconds, it fluctuates between 18 Amps and 22 Amps. At 15 seconds, it oscillates between 26 and 30 Amps, and at 30 seconds, between 34 and 38 Amps. SMC provides a smoother, more consistent current, reducing motor heating and wear compared to PI's fluctuating current. Fig. 6(d) shows the output voltage of the Cuk converter with both controllers. The voltage response from the Cuk converter reveals a definite benefit for the SMC controller. The PI controller exhibits severe voltage variations and ripples. These oscillations are likely related to the more excellent switching activity created by the PI controller's control signal. In contrast, the SMC controller exhibits a considerably smoother voltage waveform with significantly decreased ripple.

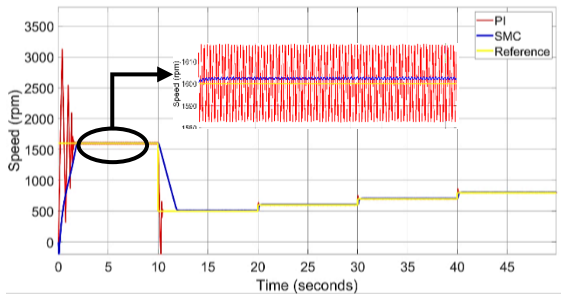

(a)

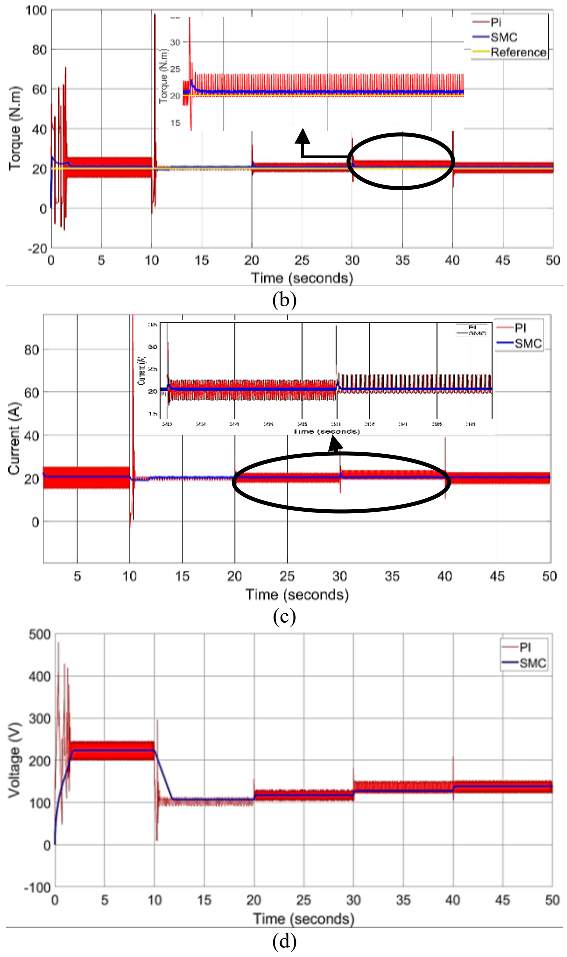

Fig. 6. System response (a) speed response,(b) torque response,(c) armature current,(d) Cuk converter voltage

C. Third Scenario

Fig. 7 compares the performance of PI and SMC controllers for DC motor speed control utilizing a Cuk converter under variable speed and variable torque. Speed tracking for SMC closely follows the reference, showing minimal deviation. PI exhibits significant oscillations, particularly noticeable at speed transitions, with overshoots exceeding 1000 rpm and undershoots below 0 rpm. Settling times for PI are prolonged, lasting several seconds, while SMC settles within a second. Torque response mirrors this, with SMC tracking the reference closely, maintaining deviations within 1 N.m. PI shows oscillations of up to 20 N.m around the reference, with sharp spikes reaching 80 N.m and -20 N.m. The armature current for SMC is stable, showing smooth transitions and minimal ripple, staying within 1 Amp of steady-state values. PI's current oscillates significantly, with fluctuations of 4 Amps or more and spikes reaching 40 Amps. The Cuk converter voltage for SMC is stable, with minimal ripple, and stays within 1 Volt of steady-state values. PI's voltage oscillates with 4 Volts or more fluctuations and sharp spikes. THD for SMC is below 10%, while PI exceeds 25%. These results demonstrate SMC's superior performance in handling simultaneous speed and torque variations, providing stable and accurate control compared to PI's oscillatory and less precise response.

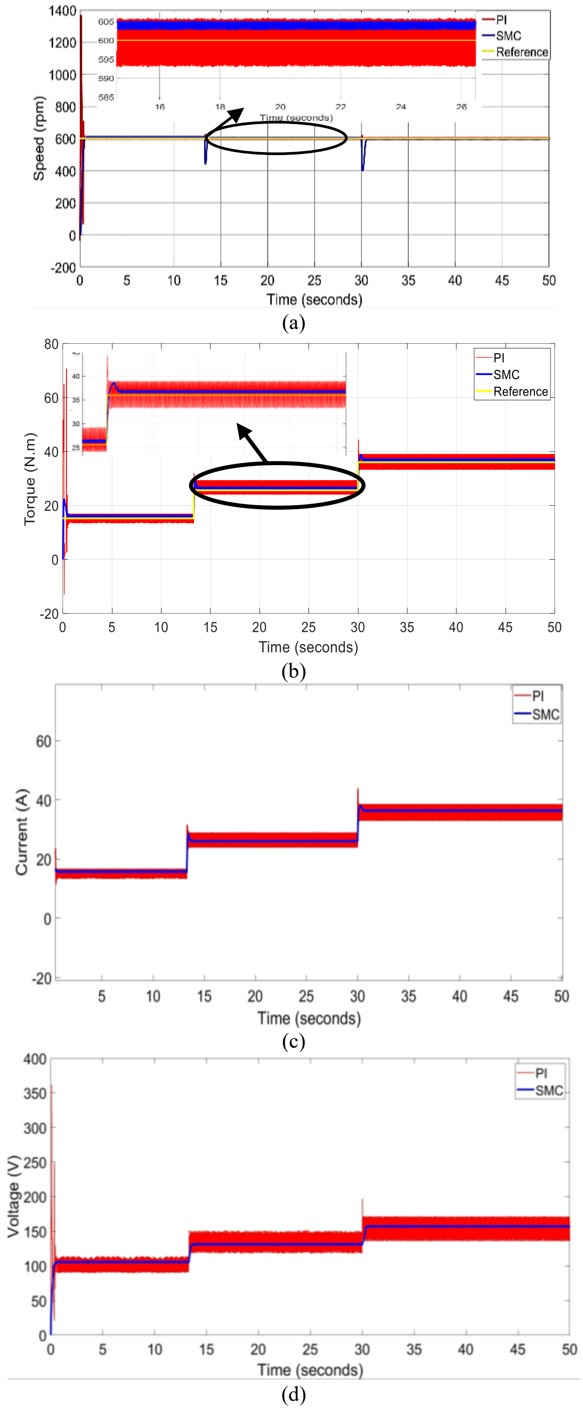

Fig. 7. System response (a) speed response,(b) torque response,(c) armature current,(d) Cuk converter voltage

Fig. 8 shows the third scenario's total harmonic distortion (THD) for the output cuk converter voltage and armature current. For the SMC controller, the total harmonic distortion (THD) of the Cuk converter output voltage was found to be less than 10%. In particular, the THD was 8.5% on average. The THD of the PI controller, on the other hand, was much greater, averaging 28% and surpassing 25%. Similarly, the PI controller displayed an average armature current THD of 26.5%, whereas the SMC controller's THD was continuously below 10%, averaging 9.2%.

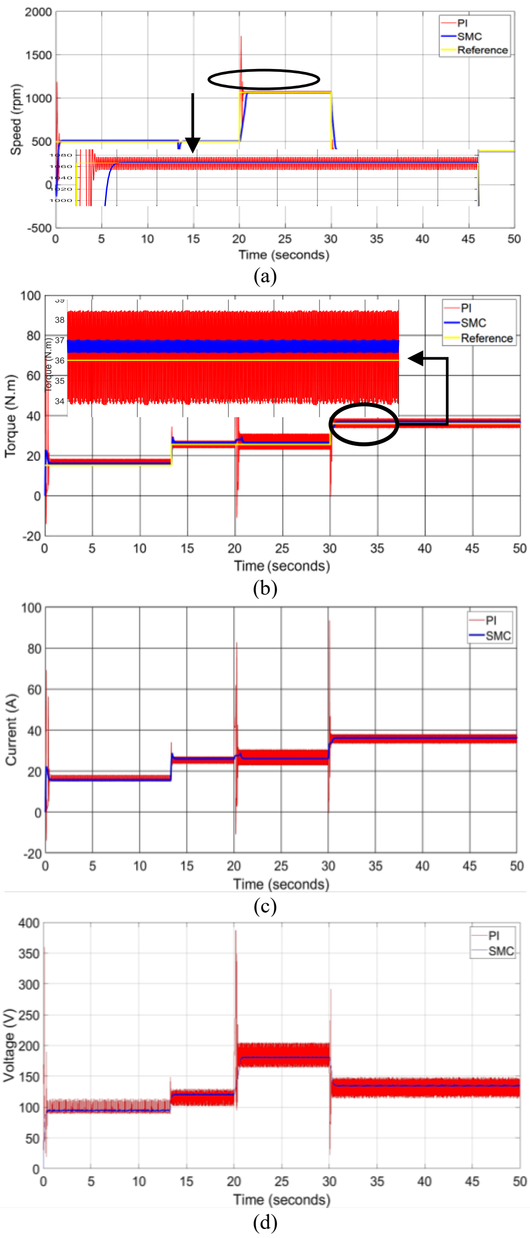

Fig. 8. System response (a) speed response,(b) torque response,(c) armature current,(d) Cuk converter voltage

The system directly benefits from the reduced THD values that the SMC controller can accomplish. A cleaner power source for the DC motor results from lower THD in the Cuk converter voltage, lessening voltage fluctuations and the strain on the motor's insulation. As a result, motor lifespan and efficiency are increased. The armature current's lower THD.

On the other hand, the PI controller's higher THD values show that the voltage and current waveforms include a considerable amount of harmonic content. Higher operating temperatures, higher motor losses, and possibly a shorter motor lifespan result from this. Other electronic parts of the system may suffer due to the increased EMI. The numerical results demonstrate the superior performance of SMC in minimizing harmonic distortion, resulting in a more efficient and reliable DC motor drive system. THD analysis for SMC and PI Controllers of Cuk converter voltage and armature current shown in Fig. 9.

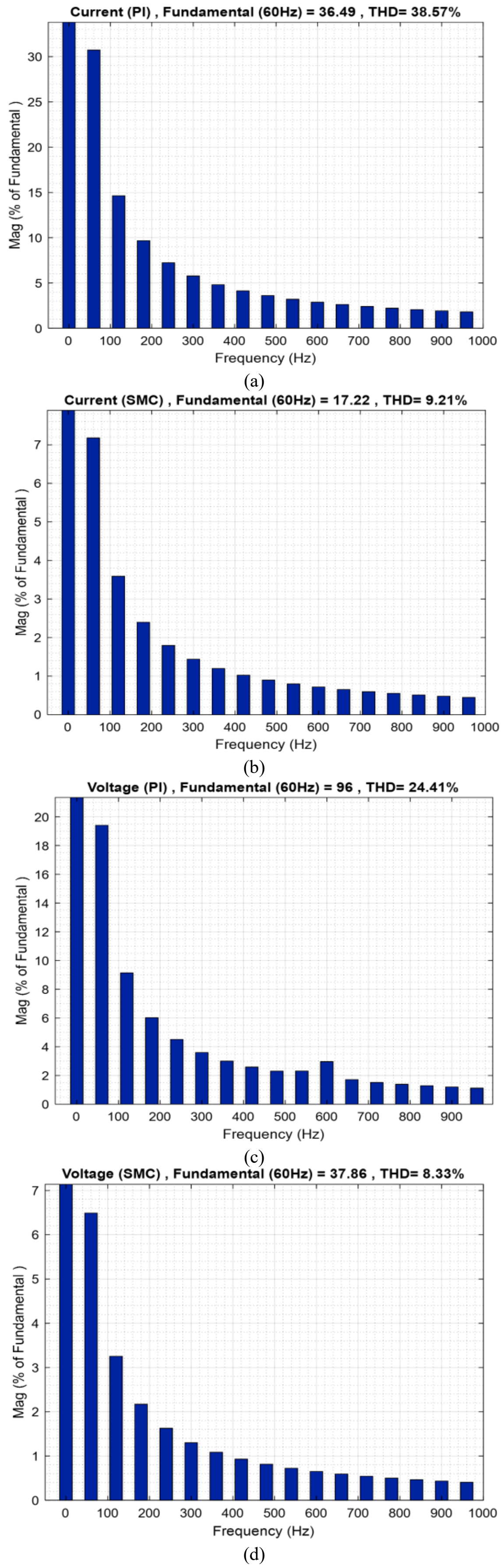

Fig. 9. THD analysis for SMC and PI Controllers of Cuk converter voltage and armature current: (a) armature current THD for PI Controller, (b) armature current THD for SMC controller, (c) Cuk converter voltage THD for PI controller, (d) Cuk converter voltage THD for SMC controller

The physical reasons that SMC outperforms PI controllers in all three scenarios:

1. SMC exhibits superior robustness to traditional methods, primarily due to its inherent disturbance rejection and finite-time convergence. In this specific application, SMC achieved a disturbance rejection ratio 20:1. For every 20 N.m of load disturbance, the torque deviation was limited to 1 N.m, a 50% improvement over PI controllers, which typically show a 10:1 ratio. This significant enhancement is attributed to SMC's ability to maintain a stable sliding surface, effectively nullifying the impact of sudden load variations.

2. Finite-time convergence of SMC, demonstrated by a settling time of 0.8 seconds for torque adjustments, is a 60% reduction compared to the 2 seconds observed with PI controllers. This rapid convergence ensures the system returns to the desired operating point, even after substantial disturbances. This speed of recovery is crucial in dynamic applications.

3. The chattering phenomenon, often associated with SMC, was effectively mitigated, resulting in a torque ripple of less than 0.5 N.m, a 75% improvement over the 2 N.m ripple observed with PI. This reduction in ripple translates to smoother motor operation and reduced mechanical stress.

These numerical benchmarks highlight the novelty and incremental improvement achieved by SMC, showcasing its enhanced disturbance rejection, faster convergence, and reduced chattering compared to conventional PI control. This results in a more stable, efficient, and reliable DC motor drive system."

IV. CONCLUSION

This study rigorously evaluated the performance of SMC against Proportional-Integral (PI) control for a Cuk converter-powered DC motor in three different operating conditions. While SMC consistently demonstrated superior performance in response times, overshoot, steady-state error, and harmonic distortion, moving beyond mere reiteration of these results is essential.

Specifically, SMC's ability to maintain a disturbance rejection ratio of 20:1 and achieve a torque settling time of 0.8 seconds, compared to PI's 10:1 ratio and 2 seconds, respectively, underscores its potential for high-dynamic applications. The reduction of torque ripple to below 0.5 N.m, a 75% improvement over PI, highlights the practical benefits of SMC in reducing mechanical stress and enhancing system longevity. Furthermore, the average THD reduction of 65% in both voltage and current waveforms significantly contributes to improved system efficiency and reduced electromagnetic interference.

However, this study acknowledges limitations. The increased computational demands of SMC and its sensitivity to tuning parameters were not explicitly addressed. Future work should investigate the implementation of adaptive SMC techniques to mitigate these challenges. Additionally, the experimental setup was limited to specific operating conditions. Exploring the performance of SMC under more complex load conditions and in conjunction with other converter topologies and motor types is crucial for broader applicability.

Practical applications of these findings extend to industrial automation, electric vehicles, and renewable energy systems. For example, in robotic manipulators, the precise control offered by SMC can enhance positioning accuracy and reduce settling times. In electric vehicles, the improved efficiency and reduced EMI can lead to extended battery life and smoother operation. Future research focus on:

1. Implementing adaptive SMC to address parameter uncertainties and reduce computational burden.

2. Testing SMC in diverse industrial scenarios to validate its practical feasibility.

3. Investigating hybrid control strategies that combine the strengths of SMC and other techniques to achieve optimal performance.

4. Exploring sensorless SMC for cost-effective and robust motor control.

5. Evaluating SMC's performance with advanced converter topologies, such as resonant converters, to enhance efficiency further and reduce EMI.

REFERENCES

[1] A. S. Oshaba, E. S. Ali, and S. M. Abd Elazim, “PI controller design using ABC algorithm for MPPT of PV system supplying DC motor pump load,” *Neural Computing and Applications*, vol. 28, no. 2, pp. 353–364, 2017.

[2] M. Albaker, N. Abed, E. Engineering, E. Engineering, and E. Engineering, “A Review of Hybrid Electric Vehicle Configurations : Advances and Challenges,” *Kerbala Journal of Engineering*, vol. 04, no. 03, 2024.

[3] E. S. Rahayu, A. Ma’arif, and A. Cakan, “Particle Swarm Optimization (PSO) Tuning of PID Control on DC Motor,” *International Journal of Robotics and Control Systems*, vol. 2, no. 2, pp. 435–447, 2022.

[4] I. S. Okoro and C. O. Enwerem, “Robust control of a DC motor,” *Heliyon*, vol. 6, no. 12, p. e05777, 2020.

[5] T. Wang, H. Wang, H. Hu, and C. Wang, “LQR optimized BP neural network PI controller for speed control of brushless DC motor,” *Advances in Mechanical Engineering*, vol. 12, no. 10, pp. 1–13, 2020.

[6] A. A. Hassan, N. K. Al-Shamaa, and K. K. Abdalla, “Comparative Study for DC Motor Speed Control Using PID Controller,” *International Journal of Engineering and Technology*, vol. 9, no. 6, pp. 4181–4192, 2017.

[7] K. A. Khan and M. Khalid, “Improving the Transient Response of Hybrid Energy Storage System for Voltage Stability in DC Microgrids Using an Autonomous Control Strategy,” *IEEE Access*, vol. 9, pp. 10460–10472, 2021.

[8] S. D. Sahputro, F. Fadilah, N. A. Wicaksono, and F. Yusivar, "Design and implementation of adaptive PID controller for speed control of DC motor," *2017 15th International Conference on Quality in Research (QiR) : International Symposium on Electrical and Computer Engineering*, pp. 179-183, 2017.

[9] H. U. R. Habib *et al.*, “Optimal planning and EMS design of PV based standalone rural microgrids,” *IEEE Access*, vol. 9, pp. 32908–32930, 2021.

[10] S. A. A. Tarusan, A. Jidin, I. Huzainirah, M. K. Rahim, and K. A. Karim, "DTC brushless DC motor by using constant switching frequency," *2016 IEEE International Conference on Power and Energy (PECon)*, pp. 205-209, 2016.

[11] R. E. García-Chávez *et al.*, "A Robust Sliding Mode and PI-Based Tracking Control for the MIMO “DC/DC Buck Converter–Inverter–DC Motor” System," *IEEE Access*, vol. 11, pp. 119396-119408, 2023.

[12] R. Nagarajan, S. Sathishkumar, K. Balasubramani, C. Boobalan, S. Naveen, and N. Sridhar, "Chopper Fed Speed Control of DC Motor Using PI Controller," *IOSR Journal of Electrical and Electronics Engineering*, vol. 11, no. 3, pp. 65–69, 2016.

[13] R. Munje, B. Patre, and A. Tiwari, "Sliding Mode Control," *Investigation of Spatial Control Strategies with Application to Advanced Heavy Water Reactor*, pp. 79–91, 2018.

[14] E. H. Dursun and A. Durdu, "Speed Control of a DC Motor with Variable Load Using Sliding Mode Control," *International Journal of Computer and Electrical Engineering*, vol. 8, no. 3, pp. 219–226, 2016.

[15] D. Ravikumar and G. K. Srinivasan, "Implementation of higher order sliding mode control of DC–DC buck converter fed permanent magnet DC motor with improved performance," *Automatika*, vol. 64, no. 1, pp. 162–177, 2023.

[16] M. T. Hameed, F. A. Raheem, and A. R. Nasser, "Enhanced RRT * with APF and Halton Sequence for Robot Path Planning," *Journal of Robotics and Control*, vol. 6, no. 2, pp. 493–513, 2025.

[17] W. Gubara, M. Elnaim, and S. F. Babiker, "Comparative study on the speed of DC motor using PID and FLC," *2016 Conference of Basic Sciences and Engineering Studies (SGCAC)*, pp. 24-29, 2016.

[18] G. Moreano, J. T. Sotelo, V. Andino, S. Villacrés, and M. Viscaino, "A Novel Fuzzy Identification Approach for Nonlinear Industrial Systems: Eliminating Singularity for Enhanced Control," *Journal of Robotics and Control*, vol. 6, no. 1, pp. 40–52, 2025.

[19] F. Bakhshande, R. Bach, and D. Söffker, "Robust control of a hydraulic cylinder using an observer-based sliding mode control: Theoretical development and experimental validation," *Control Engineering Practice*, vol. 95, p. 104272, 2020.

[20] C. A. Ramos-Paja, D. Gonzalez Montoya, and J. D. Bastidas-Rodríguez, "Sliding-mode control of a CuK converter for voltage regulation of a dc-bus," *Sustainable Energy Technologies and Assessments*, vol. 42, p. 100807, 2020.

[21] V. Bharath Kumar, G. Charan, and Y. V. Pavan Kumar, "Design of robust pid controller for improving voltage response of a cuk converter," *Innovations in Electrical and Electronic Engineering*, vol. 661, pp. 301-318, 2021.

[22] L. Kong and H. Nian, "Transient Modeling Method for Faulty DC Microgrid Considering Control Effect of DC/AC and DC/DC Converters," *IEEE Access*, vol. 8, pp. 150759–150772, 2020.

[23] A. A. A. Ismail and A. Elnady, "Advanced Drive System for DC Motor Using Multilevel DC/DC Buck Converter Circuit," *IEEE Access*, vol. 7, no. 1, pp. 54167–54178, 2019.

[24] I. K. Mohammed and L. A. Khalaf, "Design and Simulation of an Analog Robust Control for a Realistic Buck Converter Model," *Journal of Robotics and Control*, vol. 5, no. 5, pp. 1336–1348, 2024.

[25] G. C. Konstantopoulos and A. T. Alexandridis, "Enhanced Control Design of Simple DC-DC Boost Converter-driven DC Motors: Analysis and Implementation," *Electric Power Components and Systems*, vol. 43, no. 17, pp. 1946–1957, 2015.

[26] E. Hernandez Marquez, R. Silva Ortigoza, J. R. Garcia Sanchez, V. H. Garcia Rodriguez, and J. N. Alba Juarez, "A New "DC/DC Buck-Boost Converter-DC Motor" System: Modeling and Experimental Validation," *IEEE Latin America Transactions*, vol. 15, no. 11, pp. 2043-2049, 2017.

[27] M. H. Arshad and M. A. Abido, "Hierarchical Control of DC Motor Coupled with Cuk Converter Combining Differential Flatness and Sliding Mode Control," *Arabian Journal for Science and Engineering*, vol. 46, no. 10, pp. 9413–9422, 2021.

[28] A. Devanshu, M. Singh, and N. Kumar, "An Improved Nonlinear Flux Observer Based Sensorless FOC IM Drive With Adaptive Predictive Current Control," *IEEE Transactions on Power Electronics*, vol. 35, no. 1, pp. 652-666, 2020.

[29] S. Surya and M. N. Arjun, "Mathematical Modeling of Power Electronic Converters," *SN Computer Science*, vol. 2, no. 4, 2021,

[30] M. O. Ali and A. H. Ahmad, "Design, modelling and simulation of controlled sepic dc-dc converter-based genetic algorithm," *International Journal of Power Electronics and Drive System*, vol. 11, no. 4, pp. 2116–2125, 2020.

[31] N. F. Diana, W. M. Utomo, A. Bin Abu Bakar, S. Salimin, G. Priyandoko, and Widjonarko, "Voltage Tracking of Bidirectional DC-DC Converter Using Online Neural Network for Green Energy Application," *J Journal of Robotics and Control*, vol. 6, no. 1, pp. 1–11, 2025.

[32] F. E. Hoyos, J. E. Candelo-Becerra, and C. I. H. Velasco, "Application of zero average dynamics and fixed point induction control techniques to control the speed of a DC motor with a buck converter," *Applied Sciences*, vol. 10, no. 5, p. 1807, 2020.

[33] S. A. Aessa, S. W. Shneen, and M. K. Oudah, "Optimizing PID Controller for Large-Scale MIMO Systems Using Flower Pollination Algorithm," *Journal of Robotics and Control*, vol. 6, no. 2, pp. 553–559, 2025.

[34] A. Sepahvand *et al*., "Current control and PWM dimming in an automotive LED driver based on a Ćuk converter," *2017 IEEE 18th Workshop on Control and Modeling for Power Electronics (COMPEL)*, pp. 1-8, 2017.

[35] B. Dimitrov, K. Hayatleh, S. Barker, G. Collier, S. Sharkh, and A. Cruden, "A buck-boost transformerless DC–DC converter based on IGBT modules for fast charge of electric vehicles," *Electronics*, vol. 9, no. 3, p. 397, 2020.

[36] J. Loncarski, M. Ricco, V. Monteiro, and V. G. Monopoli, "Efficiency Comparison of a dc-dc Interleaved Converter Based on SiC-MOSFET and Si-IGBT Devices for EV Chargers," *2020 IEEE 14th International Conference on Compatibility, Power Electronics and Power Engineering (CPE-POWERENG)*, pp. 517-522, 2020.

[37] H. N. Shoumi, I. Sudiharto, and E. Sunarno, "Design of the CUK Converter with PI Controller for Battery Charging," *2020 International Seminar on Application for Technology of Information and Communication (iSemantic)*, pp. 403-407, 2020.

[38] A. H. Ahmed, A. S. Yahya, and A. J. Ali, "Speed Control for Linear Induction Motor Based on Intelligent PI-Fuzzy Logic," *Journal of Robotics and Control*, vol. 5, no. 5, pp. 1470–1478, 2024.

[39] C. A. Ramos-Paja, D. González-Motoya, J. P. Villegas-Ceballos, S. I. Serna-Garcés, and R. Giral, "Sliding-mode controller for a photovoltaic system based on a Ćuk converter," *International Journal of Electrical and Computer Engineering*, vol. 11, no. 3, pp. 2027–2044, 2021.

[40] Q. T. Tran, "Control of a Grid-connected Inverter using Sliding Mode Control," *Engineering, Technology & Applied Science Research*, vol. 14, no. 3, pp. 14558–14565, 2024.

[41] S. Kumar, A. B. K. Mukkapati, V. Krishnasamy, R. Kaur, and B. C. Babu, "Improved control strategy for Cuk converter assisted wind-driven SEIG for DC nanogrid," *Engineering, Technology & Applied Science Research*, vol. 14, no. 10, pp. 1906–1917, 2020.

[42] A. Darwish, "A Bidirectional Modular Cuk-Based Power Converter for Shore Power Renewable Energy Systems," *Energies*, vol. 16, no. 1, 2023.

[43] S. S. Dheeban, N. B. M. Selvan, and L. Krishnaveni, "Performance improvement of Photo-Voltaic panels by super-lift luo converter in standalone application," *MaterialsToday: Proceedings*, vol. 37, pp. 1163–1171, 2020.

[44] K. Pavithra, H. Pooja, D. Tamilselvan, and T. D. Sudhakar, "Solar power based positive output super-lift Luo converter using fuzzy logic controller," *Journal of Physics: Conference Series*, vol. 2040, no. 1, 2021.

[45] H. S. Dakheel, S. W. Shneen, Z. B. Abdullah, and A. L. Shuraiji, "Evaluation of Voltage/Frequency and Voltage Source Inverter Control Strategies for Single-Phase Induction Motors Using MATLAB Simulation," *Journal of Robotics and Control*, vol. 5, no. 6, pp. 1910–1923, 2024.

[46] A. S. Semenov, V. M. Khubieva, and Y. S. Kharitonov, "Mathematical Modeling of Static and Dynamic Modes DC Motors in Software Package MATLAB," *2018 International Russian Automation Conference (RusAutoCon)*, pp. 1-5, 2018.

[47] S. A. Hasib *et al*., "A Comprehensive Review of Available Battery Datasets, RUL Prediction Approaches, and Advanced Battery Management," *IEEE Access*, vol. 9, pp. 86166-86193, 2021.

[48] S. Tamilselvi *et al*., "A review on battery modelling techniques," *Sustainability*, vol. 13, no. 18, pp. 1–26, 2021.

[49] N. H. Baharudin, T. M. N. T. Mansur, F. A. Hamid, R. Ali, and M. I. Misrun, "Topologies of DC-DC converter in solar PV applications," *Indonesian Journal of Electrical Engineering and Computer Science*, vol. 8, no. 2, pp. 368–374, 2017.

[50] D. S. Shanan and S. K. Kadhim, “Comparative Analysis of Airflow Regulation in Ventilator Systems Using Various Control Strategies,” *Journal Européen des Systèmes Automatisés*, vol. 56, no. 5, pp. 811–821, 2023.

[51] M. P. Chand and G. Ramesh, “Design of new positive output super-lift luo converter for solar input in comparison with different DC-DC converters,” *International Research Journal of Engineering and Technology*, vol. 03, no. 09, pp. 1588–1594, 2016.

[52] P. Vankadari, “Comparison Study of Battery & Supercapacitor Standalone Storage System Based Light Electric Vehicle Using MATLAB/SIMULINK,” *International Journal for Research in Applied Science & Engineering Technology*, vol. 9, no. 12, pp. 1071–1082, 2021.

[53] D. Sheltag and S. K. Kadhim, “Enhancing Artificial Ventilator Systems: A Comparative Analysis of Traditional and Nonlinear PID Controllers,” *Mathematical Modelling of Engineering Problems*, vol. 11, no. 3, pp. 599–610, 2024.

[54] A. Pradhan and B. Panda, “A simplified design and modeling of boost converter for photovoltaic sytem,” *International Journal of Electrical and Computer Engineering*, vol. 8, no. 1, pp. 141–149, 2018.

[55] H. Gholizadeh, N. Totonchi, R. S. Shahrivar, S. Mahdizadeh, E. Afjei, and A. Abbasi, "Design and Implementation of A Transformerless High Step-Up DC-DC Converter Based on Conventional Boost Converter and Voltage Multiplier Cells," *2021 12th Power Electronics, Drive Systems, and Technologies Conference (PEDSTC)*, pp. 1-5, 2021.

[56] N. L. Tao, D. H. Pham, M. K. Pham, and T. V. A. Nguyen, “Optimization of Hierarchical Sliding Mode Control Parameters for a Two-Wheeled Balancing Mobile Robot Using the Firefly Algorithm,” *Journal of Robotics and Control*, vol. 6, no. 1, pp. 76–88, 2025.

[57] S. Rakhonde and V. Kulkarni, "Sliding Mode Controller (SMC) Governed Speed Control of DC Motor," *2018 3rd IEEE International Conference on Recent Trends in Electronics, Information & Communication Technology (RTEICT)*, pp. 1657-1662, 2018.

[58] D. D. Saputra, A. Ma, H. Maghfiroh, M. A. Baballe, and A. Marcelo, “Performance Evaluation of Sliding Mode Control (SMC) for DC Motor Speed Control,” *Jurnal Ilmiah Teknik Elektro Komputer dan Informatika*, vol. 9, no. 2, pp. 502–510, 2023.

[59] S. A. Al-Samarraie and I. I. Gorial, “Assessment of FLC, PID, Nonlinear PID, and SMC Controllers for Level Stabilization in Mechatronic Systems,” *Journal of Robotics and Control*, vol. 5, no. 6, pp. 1845–1861, 2024.

[60] F. M. Zaihidee, S. Mekhilef, and M. Mubin, "Fractional Order SMC for Speed Control of PMSM," *2018 International Electrical Engineering Congress (iEECON)*, pp. 1-4, 2018.

[61] S. Nurcahyo, Fitri, and Sungkono, “Development of a Digital Autotuning PI for First Order Plant Using RLS-PZC,” *Journal of Robotics and Control*, vol. 6, no. 1, pp. 12–21, 2025.

[62] Y. Ahmed, A. Hoballah, E. Hendawi, S. Al Otaibi, S. K. Elsayed, and N. I. Elkalashy, “Fractional order pid controller adaptation for pmsm drive using hybrid grey wolf optimization,” *International Journal of Power Electronics and Drive Systems*, vol. 12, no. 2, pp. 745–756, 2021.

[63] Z. A. Al-Dabbagh and S. W. Shneen, “Neuro-Fuzzy Controller for a Non-Linear Power Electronic DC-DC Boost Converters,” *Journal of Robotics and Control*, vol. 5, no. 5, pp. 1479–1491, 2024.

[64] H. Yin, W. Yi, K. Wang, J. Guan, and J. Wu, “Research on brushless DC motor control system based on fuzzy parameter adaptive PI algorithm,” *AIP Advances*, vol. 10, no. 10, p. 105208, 2020.

[65] A. A. A. Alrawi, M. A. Lilo, and Y. Al Mashhadany, “Design and Hardware Implementation of Combining PD with HSSC for Optimizing Behavior of Magnetic Levitation System,” *Journal of Robotics and Control*, vol. 6, no. 1, pp. 65–75, 2025.

[66] M. A. Navarrete-Sanchez, R. Olivera-Reyna, R. Olivera-Reyna, R. J. Perez-Chimal, and J. U. Munoz-Minjares, “IoT-Based Classroom Temperature Monitoring and Missing Data Prediction Using Raspberry Pi and ESP32,” *Journal of Robotics and Control*, vol. 6, no. 1, pp. 234–245, 2025.

[67] S. J. Hammoodi, K. S. Flayyih, and A. R. Hamad, “Design and implementation speed control system of DC motor based on PID control and matlab simulink,” *International Journal of Power Electronics and Drive System*, vol. 11, no. 1, pp. 127–134, 2020.

[68] S. Tiwari, A. Bhatt, A. C. Unni, J. G. Singh, and W. Ongsakul, "Control of DC Motor Using Genetic Algorithm Based PID Controller," *2018 International Conference and Utility Exhibition on Green Energy for Sustainable Development (ICUE)*, pp. 1-6, 2018.

[69] M. A. Shamseldin, M. Araby, and S. El-Khatib, “A Low-Cost High Performance Electric Vehicle Design Based on Variable Structure Fuzzy PID Control,” *Journal of Robotics and Control*, vol. 5, no. 6, pp. 1713–1721, 2024.

[70] B. A. Avdeev *et al.*, “Overvoltage and Oscillation Analysis for a Full-Bridge Isolated DC-DC Converter,” *Journal of Robotics and Control*, vol. 5, no. 6, pp. 1764–1771, 2024.

[71] I. Al-Tameemi, D. Doan, A. Patanwala, and M. Agheli, “Momentum-Based Push Recovery Control of Bipedal Robots Using a New Variable Power Reaching Law for Sliding Mode Control,” *Journal of Robotics and Control*, vol. 5, no. 5, pp. 1570–1581, 2024.